

Reacting the Unreactive: A Toolbox of Low-Temperature Solution-Mediated Reactions for the Facile Interconversion of Nanocrystalline Intermetallic Compounds

Robert E. Cable and Raymond E. Schaak*

Contribution from the Department of Chemistry, Texas A&M University, College Station, Texas 77842-3012

Received April 21, 2006; E-mail: schaak@mail.chem.tamu.edu

Most inorganic solids are unreactive at low temperatures, requiring high temperatures to disrupt their long-range bonding networks and to overcome the solid–solid diffusion barrier that is necessary to mix the reactants. Bulk metallurgical solids, including alloys and intermetallic compounds, are especially inert. Indeed, many are known for their resistance to oxidation and corrosion, even at high temperatures.¹ However, the surfaces of metallurgical compounds may be quite reactive, often forming thin layers of passivating phases.² This implies that if the surface area of metallurgical compounds is greatly increased by forming nanocrystals, their reactivity may also be greatly increased, lending themselves to chemical transformation. To date, a few metals and semiconductors have been shown to exhibit enhanced reactivity as nanocrystals. For example, Co nanocrystals can be reacted to form Co oxides, sulfides, and selenides,³ and CdSe quantum dots undergo reversible ion exchange with Ag⁺ to form Ag₂Se.⁴ However, analogous studies with alloys and intermetallic compounds, which can be structurally and compositionally more complex, have not been reported. The ability to modify the composition and structure of metallurgical solids rationally and predictably would be important, as these parameters are fundamentally tied to their physical and chemical properties.

Here we report that nanocrystals of intermetallic compounds undergo facile solution-mediated reactions to form derivative phases. Furthermore, these reactions are reversible, allowing stepwise and cyclic interconversion using a simple chemical process. We previously synthesized a library of nanocrystalline intermetallic compounds,^{5,6} and here we show that these intermetallics can also be used as reagents for the low-temperature solution synthesis of other intermetallic phases, including some that are difficult to make using direct one-pot reactions.

Nanocrystalline PtSn and AuCu were synthesized by NaBH₄ reduction of the appropriate metal salts in tetraethylene glycol (TEG), followed by heating to 245–310 °C, as described previously.^{5,6} These nanocrystalline solids were then isolated by centrifugation, washed several times, and fully characterized (see Supporting Information for details). Serving as out-of-the-bottle reagents, the nanocrystalline intermetallics were then redispersed in TEG and thermally reacted with metal salt solutions. No added surfactants, surface stabilizers, or reducing agents were used.

Figure 1 shows an overview of the chemical transformations that can be accomplished using nanocrystalline PtSn as a solid-state reagent. In the first reaction, NiAs-type PtSn is successfully converted to CaF₂-type PtSn₂ by reacting nanocrystalline PtSn with a TEG solution of SnCl₂ at 280 °C for 40 min. Figure 2a shows XRD patterns for the PtSn starting material, as well as phase-pure PtSn₂ that forms at 280 °C. While the XRD data convincingly support the conversion from PtSn to PtSn₂, the melting point of tin is 231 °C, and it is possible that molten tin could provide a localized flux to facilitate diffusion. Thus, we also studied the reaction of

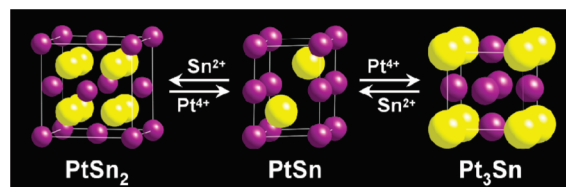


Figure 1. Schematic of the intermetallic interconversions that can be carried out using nanocrystalline PtSn as an out-of-the-bottle reagent.

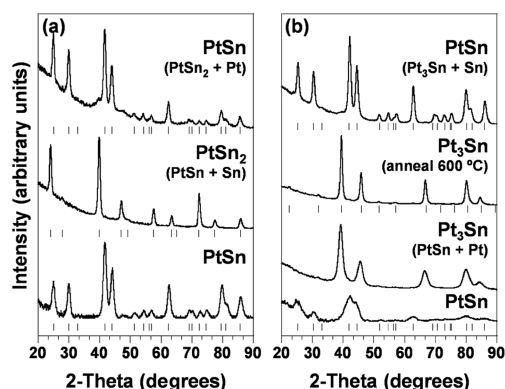


Figure 2. Powder XRD data for (a) the conversion of PtSn to PtSn₂ and the reverse reaction that converts PtSn₂ to PtSn and (b) the conversion of PtSn to Pt₃Sn, Pt₃Sn annealed at 600 °C to show the superlattice peaks, and the reverse reaction that converts Pt₃Sn to PtSn. The data shown are for sequential reactions, e.g., each reaction uses the previous product. Tick marks below each pattern represent the expected peak positions.

PtSn with Pt. PtSn can be converted to Cu₃Au-type Pt₃Sn by reacting nanocrystalline PtSn with K₂PtCl₆ at 260 °C for 20 min (Figure 2b). The diffraction pattern of Pt₃Sn has broad peaks; the small superlattice peaks at 22 and 32° 2θ, which are diagnostic of the 3:1 intermetallic, are not resolvable. However, annealing this product at 600 °C under Ar sinters the particles, making the ordering reflections resolvable. Comparison to the simulated XRD pattern for Pt₃Sn confirms that the 3:1 intermetallic was indeed formed (Figure S2).

In addition to converting PtSn to PtSn₂ and Pt₃Sn at low temperatures, the reactions are reversible. The XRD data in Figure 2a show that PtSn₂, formed by the reaction of PtSn with SnCl₂, can be converted back to PtSn by reaction with K₂PtCl₆. Likewise, Pt₃Sn, formed by reacting PtSn with K₂PtCl₆, can be converted back to PtSn by reaction with SnCl₂ (Figure 2b). The ability to reversibly interconvert these intermetallics highlights the unusual reactivity inherent in nanoscale metallurgical systems and demonstrates the level of control over composition and structure that is achievable using simple solution reactions.

The XRD data in Figure 2 show that the peak widths decrease and, consequently, the particle sizes increase as the conversion reactions progress. The increase in particle size is necessary from

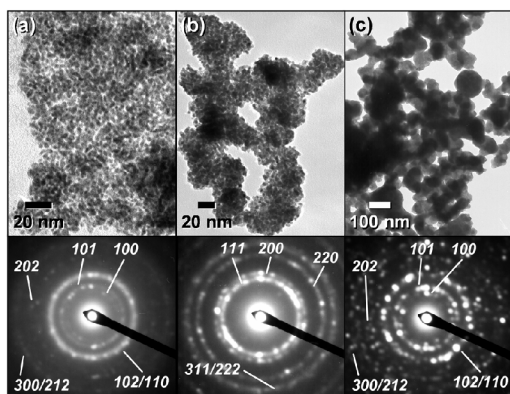


Figure 3. TEM micrographs and SAED patterns for (a) NiAs-type PtSn reagent, (b) Cu₃Au-type Pt₃Sn formed by reacting PtSn with K₂PtCl₆, and (c) NiAs-type PtSn formed by reacting Pt₃Sn with SnCl₂.

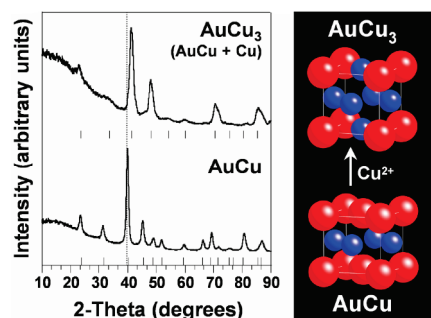


Figure 4. Powder XRD data and schematic for the conversion of nanocrystalline AuCu into AuCu₃ by reaction with Cu(C₂H₃O₂)₂·H₂O.

a mass balance perspective, because each reaction involves the addition of more material to the nanocrystals. Sintering, caused by the high-temperature solution reaction, is also likely to play a role in particle growth.

TEM images of the PtSn → Pt₃Sn → PtSn reaction sequence (Figure 3) provide additional insight into the progressive change in morphology and crystallite size, in addition to confirming the structures based on the SAED patterns. The nanoparticles of the PtSn reagent are approximately 2–5 nm (Figure 3a), which is consistent with the XRD data shown in Figure 2b. After conversion to Pt₃Sn, the particles grow to approximately 3–7 nm (Figure 3b), which is consistent with both the XRD data in Figure 2b and the expected volume expansion inherent in converting PtSn to Pt₃Sn.

Upon converting Pt₃Sn back to PtSn, the particle size increases dramatically (Figure 3c). The particle sizes are difficult to quantitate because of significant coalescence. However, when the TEM micrographs for Pt₃Sn (Figure 3b) and PtSn that were synthesized using Pt₃Sn as a reagent (Figure 3c) were compared, the PtSn particles appear to have formed from the coalescence of aggregates of smaller Pt₃Sn particles, perhaps facilitated by the reaction with low-melting tin. In addition to controlling the composition and crystal structure, this solution-mediated reaction appears to produce systematic increases in particle size, which implies that this approach could be useful for fine-tuning the morphological characteristics of nanocrystalline intermetallics.

In an effort to generalize the approach, a similar chemical transformation was attempted with the Au–Cu system. Figure 4 shows XRD data for the nanocrystalline AuCu reagent as well as AuCu₃ that was formed by reacting AuCu with Cu(C₂H₃O₂)₂·H₂O in TEG at ~315 °C. This result is particularly important, as both Au and Cu are high-melting metals (relative to Sn) and support the idea that the low-temperature diffusion is facilitated by the decreased particle size of the nanocrystals.

The discovery that nanocrystalline intermetallics undergo facile interconversion in solution has several important implications. First, it provides a robust toolkit for systematically modifying the compositions and structures of multi-metal nanocrystals, which could help fine-tune magnetic, optical, and catalytic properties and could possibly allow access to structures that are not accessible using traditional methods. Along those lines, while Pt₃Sn was readily accessible using nanocrystalline PtSn as a reagent, our attempts at synthesizing this compound using direct one-pot reactions failed. Thus, this conversion strategy produces nanocrystals of important compounds that are difficult to make by other methods. In particular, Pt₃Sn and related Pt–Sn alloys are emerging as important catalysts for fuel cell reactions,⁷ and this strategy readily produces these materials as nanocrystals. Also, while the size dependence of the reactivity and details of the reaction mechanism have yet to be established, it may be possible to use this solution approach to interconvert nanoscale intermetallics formed by other methods, including ball milling and thin film deposition. Finally, this work adds to a growing toolbox of low-temperature reactions for accessing nanocrystalline alloys and intermetallics^{8–15} and, as such, could aid in the formation of new and complex solids and challenge our thinking about the reactivity of materials traditionally considered as inert and unreactive.

Acknowledgment. This work was supported by a NSF CAREER Award (DMR-0545201), the Robert A. Welch Foundation (Grant No. A-1583), and start-up funds from Texas A&M University. Acknowledgment is also made to the Donors of the American Chemical Society Petroleum Research Fund for partial support of this research. Electron microscopy was performed at the Texas A&M Microscopy and Imaging Center.

Supporting Information Available: Experimental procedure and characterization details and additional XRD and TEM data. This material is available free of charge via the Internet at <http://pubs.acs.org>.

References

- (1) (a) Liu, C. T.; Stringer, J.; Mundy, J. N.; Horton, L. L.; Angelini, P. *Intermetallics* **1997**, *5*, 579–596. (b) Stoloff, N. S.; Liu, C. T.; Deevi, S. C. *Intermetallics* **2000**, *8*, 1313–1320.
- (2) (a) Brady, M. P.; Wrobel, S. K.; Lograsso, T. A.; Payzant, E. A.; Hoelzer, D. T.; Horton, J. A.; Walker, L. R. *Chem. Mater.* **2004**, *16*, 1984–1990. (b) Cheng, F. T.; Shi, P.; Man, H. C. *Mater. Lett.* **2005**, *59*, 1516–1520.
- (3) Yin, Y.; Rioux, R. M.; Erdonmez, C. K.; Hughes, S.; Somorjai, G. A.; Alivisatos, A. P. *Science* **2004**, *304*, 711–714.
- (4) Son, D. H.; Hughes, S. M.; Yin, Y.; Alivisatos, A. P. *Science* **2004**, *306*, 1009–1012.
- (5) Sra, A. K.; Ewers, T. D.; Schaak, R. E. *Chem. Mater.* **2005**, *17*, 758.
- (6) Cable, R. E.; Schaak, R. E. *Chem. Mater.* **2005**, *17*, 6835–6841.
- (7) (a) Schubert, M. M.; Kahllich, M. J.; Feldmeyer, G.; Huttner, M.; Hackenberg, S.; Gasteiger, H. A.; Behm, R. J. *Phys. Chem. Chem. Phys.* **2001**, *3*, 1123–1131. (b) Dupont, C.; Jugnet, Y.; Loffreda, D. *J. Am. Chem. Soc.* **2006**, *128*, published ASAP [DOI: 10.1021/ja061303h].
- (8) (a) Sra, A. K.; Schaak, R. E. *J. Am. Chem. Soc.* **2004**, *126*, 6667–6672. (b) Schaak, R. E.; Sra, A. K.; Leonard, B. M.; Cable, R. E.; Bauer, J. C.; Han, Y.-F.; Means, J.; Teizer, W.; Vasquez, Y.; Funck, E. S. *J. Am. Chem. Soc.* **2005**, *127*, 3506–3515.
- (9) Leonard, B. M.; Bhuvanesh, N. S. P.; Schaak, R. E. *J. Am. Chem. Soc.* **2005**, *127*, 7326–7327.
- (10) Haber, J. A.; Gunda, N. V.; Balbach, J. J.; Conradi, M. S.; Buhro, W. E. *Chem. Mater.* **2000**, *12*, 973–982.
- (11) Bonnemant, H.; Brijioux, W.; Hofstadt, H. W.; Ould-Ely, T.; Schmidt, W.; Wassmuth, B.; Weidenhaler, C. *Angew. Chem., Int. Ed.* **2002**, *41*, 599–603.
- (12) Vondrova, M.; Majsztrik, P. W.; Gould, S.; Bocarsly, A. B. *Chem. Mater.* **2005**, *17*, 4755–4757.
- (13) Schlecht, S.; Erk, C.; Yosef, M. *Inorg. Chem.* **2006**, *45*, 1693–1697.
- (14) Roychowdhury, C.; Matsumoto, F.; Mutolo, P. F.; Abruna, H.; DiSalvo, F. J. *Chem. Mater.* **2005**, *17*, 5871–5876.
- (15) Karkamkar, A. J.; Kanatzidis, M. G. *J. Am. Chem. Soc.* **2006**, *128*, 6002–6003.

JA0627996